Interference Effects on Resonance Raman Excitation Profiles Caused by Two Electronic Excited States

Kyeong-Sook Kim Shin and Jeffrey I. Zink*

Contribution from the Department of Chemistry and Biochemistry, University of California, Los Angeles, Los Angeles, California 90024. *Received February 5, 1990*

Abstract: Resonance Raman excitation profiles in resonance with a given electronic excited state can be strongly affected by the other excited states of the molecule. The best known example is resonance deenhancement. The effects of multiple electronic excited states on excitation profiles are calculated for the first time by using the time-dependent theory of resonance Raman spectroscopy. Trends are derived from calculations on a two-state model system. The effect on the excitation profiles of the energy separation between the two states, the transition dipole moments of the two states, the displacements of the normal coordinates in the two states, and the damping factors in the two states are calculated and interpreted. The theory is applied to the resonance Raman excitation profiles of $Co(en)_3^{3+}$, $PdBr_4^{2-}$, $Ru_2(O_2CCH_3)_4Cl$, and $W(CO)_4$(*i*-PrDAB). The profiles of the first three molecules exhibit resonance deenhancement in the region of an absorption band with a relatively small transition dipole moment that is near in energy to a band with a large transition dipole moment. The tungsten compound illustrates the effect of two nearby states with similar transition dipole moments. The molecular properties including the distortions in the excited states of these molecules are discussed.

I. Introduction

Resonance Raman spectroscopy is a powerful tool for determining distortions that molecules undergo upon excitation to excited states and for experimentally obtaining excited-state potential surfaces.[1] Resonance Raman excitation profiles are especially useful when electronic absorption and emission spectra are unstructured. The electronic spectra of large molecules in condensed media contain information about all of the normal modes of the molecule whose potential surface minima are displaced from the minimum of the ground electronic state. However, the spectra of molecules with many displaced normal modes are frequently very congested, resulting in an unresolved envelope. In contrast, resonance Raman profiles can be used to obtain information about individual modes because the excited-state information is "filtered" through the specific normal mode being examined. Detailed information about displacements in multimode systems has been obtained.[2-10]

The simplest calculations and interpretations are usually based on the assumption that the excited state of interest is not influenced by other excited electronic states. The presence of one or more nearby states complicates the interpretation. In many cases, the state of interest has a transition dipole moment that is much larger than those of nearby states. Because the resonance Raman cross section is related to the square of the transition dipole moment, the transition having the greatest dipole moment may dominate the resonance profiles.

If the excited state of interest has a relatively small transition dipole moment and if a nearby excited state has a large dipole, then interference between the two states may lead to unusual effects such as resonance deenhancement.[11-16] Spiro et al. identified the origin of the deenhancement and successfully interpreted the effect by using the Kramers-Heisenberg-Dirac (KHD) formalism.[14] This formalism is cumbersome for even one mode and does not lend itself to easy calculations. Another case in which interference between the states will lead to unusual excitation profiles is when two excited-state absorption bands overlap and have similar dipole moments. This situation, while common, has not been analyzed.

In this paper, we use the time-dependent theory of Lee, Tannor, and Heller to interpret and calculate excitation profiles resulting from interferences between multiple electronic excited states. The time-dependent theory provides both a clear physical picture and computational simplicity.[17-20] The important factors that govern the interference effect are considered. Model calculations are done for two different cases. In the first case, two electronic excited states are well-separated in energy and the transition dipole moment of the second excited state is much higher than that of the first excited state. In the second case, two electronic excited states are close in energy and the transition dipole moment of the second excited state is comparable to that of the first excited state. The time-dependent theory is applied to the excitation profiles of $Co(en)^{3+}$,[14] $PdBr_4^{2-}$,[14] $Ru_2(O_2CCH_3)_4Cl$,[21] and $W(CO)_4$(*i*-PrDAB).[22] The distortions of these complexes in the excited states are estimated.

II. Theory

The time-dependent theory of resonance Raman spectroscopy has been discussed and applied previously in detail when only one electronic excited state is involved.[4,19] In this paper, the effect of a second excited electronic state on the Raman excitation profile of the first state will be considered in detail.

The resonance Raman scattering cross section for many electronic excited surfaces is given by[20]

$$\alpha_{fi} = \frac{i}{\hbar}\int_0^\infty \sum_{r=1}^{n} \langle \phi_f | \phi(t) \rangle_r \exp\{i(\omega_i + \omega_1)t\}\, dt \qquad (1)$$

(1) Clark, R. J. H., Hester, R. E., Ed. *Advances in Infrared and Raman Spectroscopy*; Wiley: Chichester, 1975-1989; Vols. 1-17 and references therein. Clark, R. J. H.; Dines, T. J. *Angew. Chem., Int. Ed. Engl.* **1986**, *25*, 13, and references therein.
(2) Shin, K. S.; Clark, R. J. H.; Zink, J. I. *J. Am. Chem. Soc.* **1989**, *111*, 4244.
(3) Shin, K. S. K.; Zink, J. I. *Inorg. Chem.* **1989**, *28*, 4358.
(4) Shin, K. S.; Clark, R. J. H.; Zink, J. I. *J. Am. Chem. Soc.* **1990**, *112*, 3754.
(5) Clark, R. J. H.; Stewart, B. *J. Am. Chem. Soc.* **1981**, *103*, 6593.
(6) Clark, R. J. H.; Dines, T. J.; Kurmoo, M. *Inorg. Chem.* **1983**, *22*, 2766.
(7) Clark, R. J. H.; Dines, T. J.; Doherty, J. M. *Inorg. Chem.* **1985**, *24*, 2088.
(8) Clark, R. J. H.; Dines, T. J.; Wolf, M. L. *J. Chem. Soc., Faraday Trans. 2* **1982**, *78*, 679.
(9) Clark, R. J. H.; Dines, T. J.; Proud, G. P. *J. Chem. Soc., Dalton Trans.* **1983**, 2019.
(10) Myers, A. B.; Pranata, K. S. *J. Phys. Chem.* **1989**, *93*, 5079. Myers, A. B.; Mathies, R. A.; Tannor, D. J.; Heller, E. J. *J. Chem. Phys.* **1982**, *77*, 3857.
(11) Bosworth, Y. M.; Clark, R. J. H. *J. Chem. Soc., Dalton Trans.* **1974**, 1749. Bosworth, Y. M.; Clark, R. J. H.; Turtle, P. C. *J. Chem. Soc., Dalton Trans.* **1975**, 2027.
(12) Fodor, S. P. A.; Copeland, R. A.; Grygon, C. A.; Spiro, T. G. *J. Am. Chem. Soc.* **1989**, *111*, 5509.
(13) Nafie, L. A.; Pastor, R. W.; Dabrowiak, J. C.; Woodruff, W. H. *J. Am. Chem. Soc.* **1976**, *98*, 8007.
(14) Stein, P.; Miskowski, V.; Woodruff, W. H.; Griffin, J. P.; Werner, K. G.; Gaber, B. P.; Spiro, T. G. *J. Chem. Phys.* **1976**, *64*, 2159.
(15) Zgierski, M. Z. *J. Raman Spectrosc.* **1977**, *6*, 53.
(16) Schick, G. A.; Bocian, D. F. *J. Raman Spectrosc.* **1981**, *11*, 27.
(17) Lee, S. Y.; Heller, E. J. *J. Chem. Phys.* **1979**, *71*, 4777.
(18) Williams, S. O.; Imre, D. G. *J. Phys. Chem.* **1988**, *92*, 3363.
(19) Heller, E. J.; Sundberg, R. L.; Tannor, D. *J. Phys. Chem.* **1982**, *86*, 1822.
(20) Tannor, D.; Heller, E. J. *J. Phys. Chem.* **1982**, *77*, 202.
(21) Clark, R. J. H.; Ferris, L. T. H. *Inorg. Chem.* **1981**, *20*, 2159.
(22) Servaas, P. C.; Dijk, H. K. V.; Snoeck, T. L.; Stufkens, D. J.; Oskam, A. *Inorg. Chem.* **1985**, *24*, 4494.

0002-7863/90/1512-7148$02.50/0

where $\langle\phi_f| = \langle\chi_f|\mu$ is the final vibrational state χ_f of the ground electronic surface multiplied by the transition dipole moment μ; $|\phi(t)\rangle = \exp(-iH_{ex}t/\hbar)|\phi\rangle$ is a moving wavepacket propagated on the rth electronic excited state by the excited-state Hamiltonian; $|\phi\rangle = \mu|\chi\rangle$ is the initial vibrational state of the ground electronic surface multiplied by the electronic transition dipole moment; $\hbar\omega_i$ is the zero-point energy of the ground electronic surface; and $\hbar\omega_l$ is the energy of the incident radiation.

If it is assumed that (a) the potential surfaces are harmonic, (b) the normal coordinates are not mixed in the excited state, (c) the transition dipole moment μ is constant, and (d) the force constants do not change in the excited state, then the overlap for the rth excited state has the simple form

$$\langle\phi_f|\phi(t)\rangle_r = \mu_r^2\prod_{k_r}\left\{\exp\left[-\frac{\Delta_{kr}^2}{2}(1-\exp(-i\omega_{kr}t))-\frac{i\omega_{kr}t}{2}\right]\times (1-\exp(-i\omega_{kr}t))^{n_{kr}}\frac{(-1)^{n_{kr}}\Delta_{kr}^{n_{kr}}}{(2^{n_{kr}}n_{kr}!)^{1/2}}\right\}\exp(-i\omega_{0r}t-\Gamma_r t) = \mu_r^2 O_r \quad (2)$$

where μ_r is the constant transition dipole moment of the rth excited state, ω_{0r} is the energy of the zero–zero electronic transition of the rth electronic excited state (cm^{-1}), ω_{kr} and Δ_{kr} are, respectively, the vibrational frequency (cm^{-1}) and the displacement of the kth normal mode in the rth excited state, n_{kr} is the vibrational quantum number of the kth normal mode in the ground electronic state (n_{kr} = 0, 1, 2, etc.), and Γ_r is the damping factor of the rth electronic excited state.

For example, if there are only two electronic excited states under consideration, the resonance Raman cross section is

$$\alpha_{fi} = \frac{i}{\hbar}\int_0^\infty(\mu_1^2O_1+\mu_2^2O_2)\exp\{i(\omega_i+\omega_l)t\}\,dt \quad (3)$$

where μ_1 and μ_2 are the transition dipole moments of the first and the second excited states, respectively, and O_1 and O_2 are the overlaps for the first and the second excited states, respectively. The total overlap (of which half Fourier transform is the Raman scattering cross section in the frequency domain) is obtained by adding the transition dipole moment weighted overlaps from each excited state. The Raman intensity $I_{i\to f}$ into a particular mode f is

$$I_{i\to f} \propto \omega_l\omega_s^3|\alpha_{fi}|^2 \quad (4)$$

where ω_s is the frequency of the scattered radiation.

It is simple to extend the theory to three or more excited states. The quantity μ^2O for each additional state is added to the integrand in eq 3, the half Fourier transform is obtained, and the intensities are calculated by square of the Raman cross section.

III. Analysis of the Influence of Two Excited States on Each Other

The purpose of the calculations described in detail in this section is to numerically determine the trends in resonance Raman profiles caused by two or more excited electronic states. In order to focus on the trends, the case of two excited states will be examined. As will be shown in this section, the important physical quantities are the energy separation of the two states ΔE, the relative transition dipole moments μ of the two excited states, the displacements Δ of the potential surfaces from the minimum of the ground state along the normal modes, and the damping factor Γ.

The general feature that is apparent in all of the resonance Raman profiles is that the electronic state with the largest dipole moment μ dominates the profile. This well-known fact results from eqs 3 and 4, which show that the Raman intensity is proportional to the fourth power of the transition dipole.[1] Thus, in a resonance Raman excitation profile through a region containing two electronic excited states, the presence of the state with a relatively small μ will hardly affect the profile obtained in resonance with the state having a much larger μ. However, detailed examination of the profile in resonance with the state with the small μ will in general show unusual effects caused by the influence of the second state. The best known effect is "resonance deenhancement", in which a minimum in the excitation profile may be found near the wavenumber of the maximum of the absorption band.[11-16] It must be emphasized that the intensities involved in the deenhancement region of the total excitation profile are small compared to those in the region of resonance with the state having the higher μ.

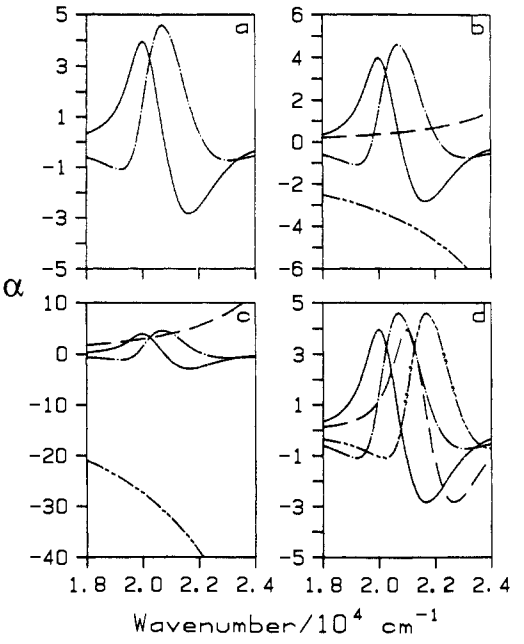

Figure 1. Real and imaginary parts of the resonance Raman scattering cross section (α) for one electronic state (a) and two states (b–d). The real (— for the first excited state, -- for the second excited state) and imaginary (-·- for the first excited state, ---- for the second excited state) parts for the 700-cm^{-1} mode are shown when (a) only the first excited state is considered (μ_2^2 = 0), (b) $\mu_1^2:\mu_2^2$ = 1:60, (c) $\mu_1^2:\mu_2^2$ = 1:500, and (d) $\mu_1^2:\mu_2^2$ = 1:1. In all cases, the values of the parameters for the first excited state are the following: Δ for the 500-cm^{-1} mode, 1.0; Δ for the 700-cm^{-1} mode, 1.0; E_{00}, 20 000 cm^{-1}; Γ, 700 cm^{-1}. For (b) and (c), the values of the parameters for the second excited state are as follows: Δ for the 500-cm^{-1} mode, 1.0; Δ for the 700-cm^{-1} mode, 1.0; E_{00}, 30 000 cm^{-1}; Γ, 700 cm^{-1}. For (d), E_{00} is 21 000 cm^{-1} and the rest of the parameters for the second excited state are the same as those in (b) and (c).

The origin of the effects to be discussed is explained by individually interpreting the real and the imaginary parts of the resonance Raman scattering cross section (α) (the square of which is proportional to the resonance Raman intensity). Consider first these parts from one electronic state

$$\alpha_{fi} = \frac{i}{\hbar}\int_0^\infty \mu_1^2O_1\exp\{i(\omega_i+\omega_l)t\}\,dt \quad (5)$$

These parts are plotted in Figure 1a. The imaginary part (-·-) peaks at the position of the maximum of the absorption band, whereas the real part (—) changes sign at that wavenumber. In Figure 1, these features occur at 20 800 cm^{-1}. The square of the sum of these two components gives the excitation profile for the first state, which is shown in Figure 2b (solid line). A second important feature is the low-energy portion of the curves. At the low-energy side of α, the real and the imaginary parts have opposite signs. In this energy region, the magnitudes of these parts increase slowly and smoothly as the energy of the excitation wavenumber increases. The signs of the real and imaginary parts shown in Figure 1a are those resulting from a positive displacement of the potential surface along the normal mode shown. The relative magnitudes of the real and imaginary parts are also quite different in the low-energy region. The magnitude of the imaginary part is significantly greater than that of the real part.

In order to calculate the effect of a second electronic excited state, its real (---) and imaginary (-··-) parts are added to those of the first state, as shown in eq 3 and Figure 1b. A second electronic excited state with a higher energy than that of the first state contributes the low-energy tail of its real and imaginary parts

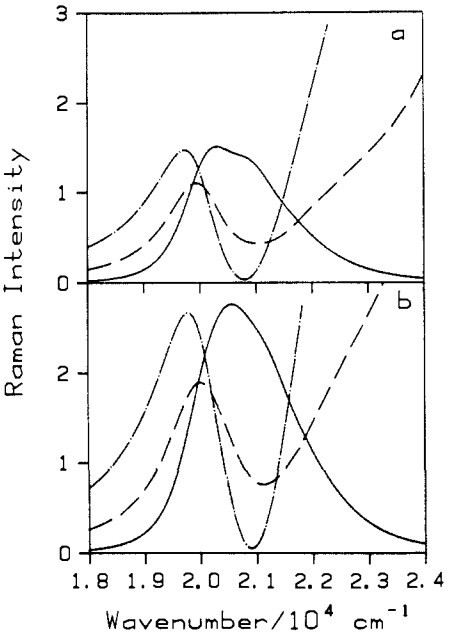

Figure 2. Resonance Raman excitation profiles illustrating the resonance deenhancement for (a) the 500- and (b) the 700-cm^{-1} modes when $\mu_1^2:\mu_2^2$ = 1:30 (--) and 1:60 (-·-). The solid line is for the first excited state only (μ_2 = 0). The displacements are 1.0 for the two modes and Γ = 700 cm^{-1} in both excited states. $E_{00}(1)$ = 20000 cm^{-1}; $E_{00}(2)$ = 30000 cm^{-1}.

to the components of the first state. The contribution of its components in the energy region of the first excited state may be negligible if the second state is much higher in energy than the first state and its transition dipole moment is not too large. However, its tail may be similar in magnitude to the components of the first state if it is near in energy and its μ is large. This situation is shown in Figure 1b. In the 20800-cm^{-1} region, the magnitude of the imaginary part of the tail from the high-energy state is about equal in magnitude but opposite in sign to the imaginary part of the low-energy state. These components destructively interfere. The real part of the tail is smaller in magnitude and does not profoundly interfere with the real part of the low-energy state. The square of the sum of all of the components gives rise to very low Raman scattering at 20800 cm^{-1}, which is shown in Figure 2b (-·-), and the destructive interference is the explanation of the deenhancement. If the second excited state is closer in energy to the first or if its μ is much larger, then the components of its tail dominate as shown in Figure 1c and the interference effects are small. The profile is dominated by the second excited state, and the minimum and the local maximum in the region of the first excited state are barely discernible.

Figure 1d shows the real and imaginary parts of two electronic states when the energy separation between the states is small and the transition dipole moments are similar. Under these conditions, the interference effects are complicated and usually need to be analyzed on a case by case basis. Several interesting results of this type of interaction will be discussed in section B. It is important to note that the relative Raman intensity in resonance with the first excited state is 4×10^5 times smaller than that in resonance with the second excited state when $\mu_1^2:\mu_2^2$ = 1:500.

From the above descriptions and eqs 3 and 4, the important quantities in the analysis of interference effects in excitation profiles are the energy separations between the excited states and the transition dipole moments of the states. In addition, the displacements Δ and the damping factor Γ for each of the excited states will play an important part in determining the shapes of the profiles. The effects of all of these quantities on the profiles are individually examined in the following sections.

A. Two Excited States Are Well-Separated in Energy, and the Transition Dipole Moment of the Second Excited State Is Much Higher Than That of the First Excited State. In this section, two excited states that are separated by 10000 cm^{-1} are considered: $E_{00}(1)$ = 20000 cm^{-1} and $E_{00}(2)$ = 30000 cm^{-1}. The excitation

Table I. Values of the Parameters Used in the Calculations

first excited state		second excited state	
ω_k, cm^{-1}	Δ_k[a]	ω_k, cm^{-1}	Δ_k[a]
500	1.0	500	1.0
700	1.0	700	1.0
Resonance Deenhancement (Section III.A)			
$E_{00}(1)$ = 20000 cm^{-1}		$E_{00}(2)$ = 30000 cm^{-1}	
Γ_1 = 700 cm^{-1}		Γ_2 = 700 cm^{-1}	
μ_1^2		μ_2^2	
Nearby States (Section III.B)			
$E_{00}(1)$ = 20000 cm^{-1}		$E_{00}(2)$ = 21000 cm^{-1}	
Γ_1 = 700 cm^{-1}		Γ_2 = 700 cm^{-1}	
μ_1^2		μ_2^2	

[a] The displacements are dimensionless.

profile in resonance with the first excited state is examined in detail. A molecule that has two vibrational modes with frequencies of 500 and 700 cm^{-1} is used as the example in the following discussion.

Effect of μ. The effect of the transition dipole moment μ of the second excited state on the resonance Raman intensity of the first excited state is the focus of this section. In order to focus on the effect of μ, the displacements of the two modes and the damping factors in the two excited states are kept the same. Only the ratio of μ's of the two excited states is varied. The displacements used in the examples are +1.0 for both the 700- and 500-cm^{-1} modes. The damping factor is 700 cm^{-1} for both excited states.

The resonance Raman excitation profiles for the 500- mode and the 700-cm^{-1} mode in the energies between 18000 and 24000 cm^{-1} are shown in parts a and b of Figure 2, respectively. They are calculated by using the parameters in Table I. The solid line shows the excitation profile for the first excited state in the absence of a second excited state. The dashed line is the excitation profile when $\mu_1^2:\mu_2^2$ = 1:30, and the dash–dotted line is the excitation profile when $\mu_1^2:\mu_2^2$ = 1:60. The excitation profile shown by the solid line in Figure 2 is the square of the resonance Raman scattering cross section α shown in Figure 1a. The relative intensities of the 500- and the 700-cm^{-1} modes are about the same, even though the ratio of μ's is changed. When the transition dipole moment of the second excited state is low, the resonance Raman excitation profile is dominated by the first excited state because the contribution of the second excited state to the total α is very small. As the transition dipole moment of the second excited state increases, the magnitude of α of the second excited state in the resonant region becomes comparable to that of the first excited state. Therefore, there is a strong interference effect from the second excited state. In general, the consequence of this interference effect is that the intensity of the excitation profile on the low-energy side of the local maximum increases and the local maxima shift to lower energy compared to that of the excitation profile of the first excited state only. When $\mu_1^2:\mu_2^2$ = 1:60, the minimum of the excitation profile of the first excited state occurs at the maximum of the absorption band of the first excited state.

Effect of Δ. Both the magnitudes and the signs of the displacements of the potential surfaces of the second excited state along the normal coordinates have profound effects on the excitation profiles in resonance with the first excited state. The large influence of the sign is unusual; the sign usually cannot be determined from Raman data because the terms involving the displacements are squared in the equations for calculating the intensities. All of the effects discussed here can be understood in terms of the constructive or destructive interference between the real and imaginary parts of α. In order to illustrate these effects of Δ, this section is divided into three parts: general effects and considerations, specific effects of the sign of Δ, and specific effects of the magnitudes of Δ. The relative Raman intensities of the modes are greatly affected not only by the displacements in the second excited state but also by those in the first excited state. In order to focus on the effect of the Δ's of the second excited state on the profiles in resonance with the first excited

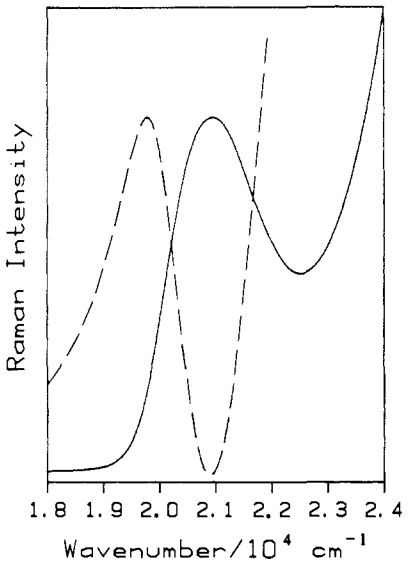

Figure 3. Resonance Raman excitation profiles illustrating the effect of the sign of the displacement in the second excited state for the 700-cm^{-1} mode. The dashed line is the calculated profile when the displacements of the 700- and 500-cm^{-1} modes are 1.0 in the two excited states. The solid line is the calculated profile when the displacements of the 700- and 500-cm^{-1} modes are +1.0 in the first excited state and −1.0 in the second excited state. $E_{00}(1)$ = 20 000 cm^{-1}, $E_{00}(2)$ = 30 000 cm^{-1}, and Γ = 700 cm^{-1} for the two excited states. $\mu_1^2:\mu_2^2$ = 1:60.

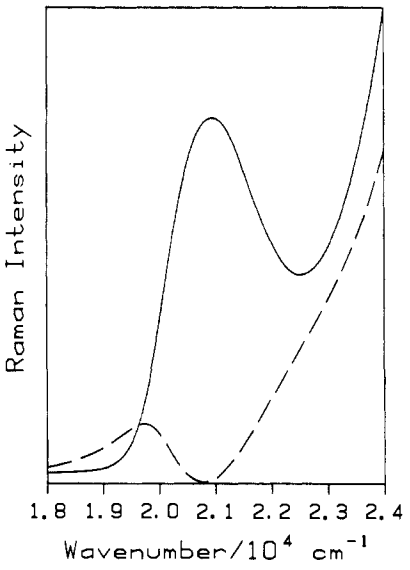

Figure 4. Presence of resonance deenhancement in the excitation profile of the 500-cm^{-1} mode (--) and its absence in that of the 700-cm^{-1} mode (—) caused by the difference in the sign of the displacements in the second excited state. The values of the parameters for the first excited state are the following: Δ for the 500-cm^{-1} mode, 1.0; Δ for the 700-cm^{-1} mode, 1.0; E_{00}, 20 000 cm^{-1}; Γ, 700 cm^{-1}. The values of the parameters for the second excited state are as follows: Δ for the 500-cm^{-1} mode, 1.0; Δ for the 700-cm^{-1} mode, −1.0; E_{00}, 30 000 cm^{-1}; Γ, 700 cm^{-1}. $\mu_1^2:\mu_2^2$ = 1:60.

state, the $\mu_1^2:\mu_2^2$ is fixed to 1:60 where the resonance deenhancement effect is most prominent. The displacements in the first excited state and the damping factors in the two excited states are also fixed. The only variables are the displacements in the second excited state.

General Effects of Changing Δ. There are two important trends in the excitation profiles as the displacements of the modes in the second excited state are increased. First, as the displacements in the second excited state increase, the local maximum in the profile through the first state shifts to lower energy and the intensity in the region on the high-energy side to the local maximum decreases; i.e., it shows more pronounced resonance deenhancement. The reason for this trend is the increase of the imaginary part of α from the second state caused by the bigger displacement, which contributes more destructively to the imaginary part of the α of the first excited state. Second, the relative Raman intensities of the two modes remain constant as Δ changes. This constancy is retained as long as the ratio of Δ's between the two modes is about the same as that in the first excited state.

Effects of Sign. When the signs of the displacements of the modes in the second excited state are changed, the shapes of the excitation profiles are dramatically different even though the magnitudes of the displacements are the same. Two examples illustrate this effect.

First, the signs of both of the two modes in the second excited state are opposite to those in the first excited state. The excitation profiles of the 700-cm^{-1} mode with the displacements of the two modes equal to −1.0 (—) in the second excited state are shown in Figure 3. These profiles are compared with those calculated for displacement of +1.0 (---) in the second excited state. The excitation profiles for the negative sign show no resonance deenhancement, even though the only difference in parameters is the negative value of the displacements in the second excited state. The shapes of the excitation profiles are about the same as those when no second excited state is considered. The relative intensity between the two modes is the same as long as the ratio of Δ's in the second excited state is the same as that in the first excited state.

Second, the displacement of one of the modes in the second excited state has the sign opposite to that in the first excited state and the other has the same sign. The excitation profiles for the 700-cm^{-1} mode (—) and 500-cm^{-1} mode (---) are shown in Figure 4 when the displacement in the second state is −1.0 for the 700-cm^{-1} mode and +1.0 for the 500-cm^{-1} mode. The excitation profile for the 700-cm^{-1} mode (the one for which the displacement in the second excited state has opposite sign to that in the first excited state) does not show the resonance deenhancement, whereas the excitation profile for the 500-cm^{-1} mode does show the resonance deenhancement.

Effects of Different Ratios of Δ's in the Second Excited State. The relative Raman intensities between the modes are dependent on the ratio of the displacements in the second excited state, even though the displacements in the first excited state are kept the same. As discussed in the previous section, the relative intensities between the modes are about the same as long as the ratio of the displacements in the second excited state is the same as that of the first excited state. When the ratio of Δ's in the second excited state is different from that in the first excited state, generally the local maxima and minima in the excitation profiles for the modes occur at different energy positions. The relative Raman intensity of a particular mode to that of the other modes in the resonant state increases as the displacement of that particular mode increases in the second excited state. There are so many possible combinations to consider that it is not simple to deduce general rules. It is instructive to consider two extreme cases. The first is the case when one of the modes has a very big displacement in the second excited state and the other does not. The second is the case when both modes have very large displacements and the ratio of Δ's of the two modes are different in the second excited state.

When one of the modes has a very big displacement and the other mode has a very small displacement in the second excited state, the shapes of the excitation profiles for the modes are quite different, even though both modes have the same displacements in the first excited state. Figure 5 shows the excitation profiles for the 700-cm^{-1} mode (—) and 500-cm^{-1} mode (---) when the displacement is 0.2 for the 700-cm^{-1} mode and 2.0 for the 500-cm^{-1} mode in the second excited state. The rest of the parameters are the same as those in Table I. The excitation profile of the 500-cm^{-1} mode shows very strong resonance deenhancement, whereas that of the 700-cm^{-1} mode does not. Because the magnitude of α of the second excited state from the 700-cm^{-1} mode is much smaller than that for the 500-cm^{-1} mode, the interference effect is smaller and the excitation profile of the 700-cm^{-1} mode is about the same as that of the first excited state only. However, the magnitude

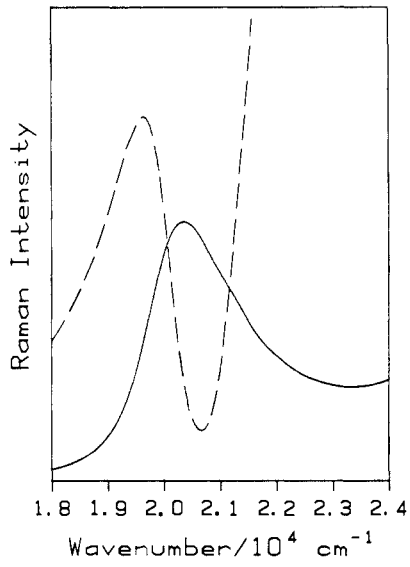

Figure 5. Absence of resonance deenhancement in the excitation profile of the 700-cm^{-1} mode (—) caused by a small displacement in the second excited state. Resonance deenhancement is observed in the profile of the 500-cm^{-1} mode (--). The values of the parameters for the first excited state are the following: Δ for the 500-cm^{-1} mode, 1.0; Δ for the 700-cm^{-1} mode, 1.0; E_{00}, 20 000 cm^{-1}; Γ, 700 cm^{-1}. The values of the parameters for the second excited state are as follows: Δ for the 500-cm^{-1} mode, 2.0; Δ for the 700-cm^{-1} mode, 0.2; E_{00}, 30 000 cm^{-1}; Γ, 700 cm^{-1}. $\mu_1^2:\mu_2^2$ = 1:60.

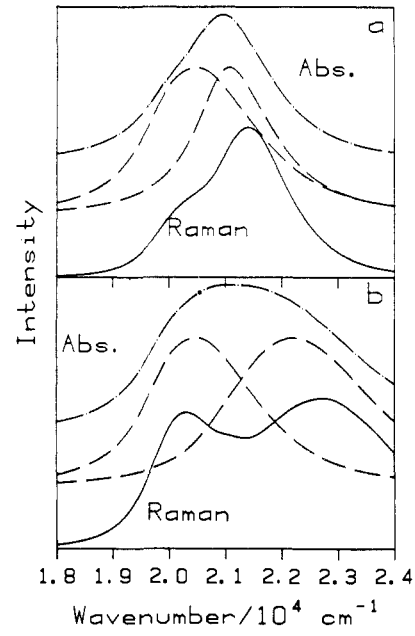

Figure 6. Resonance Raman excitation profiles for the 700-cm^{-1} mode (—) when two electronic excited states are close in energy. The displacements of the 500- and the 700-cm^{-1} modes are (a) 0.5 and (b) 1.5 in the second excited state. For (a) and (b), the displacements of the two modes in the first excited state are 1.0. Γ = 700 cm^{-1} for the two excited states, $\mu_1^2:\mu_2^2$ = 1:1, $E_{00}(1)$ = 20 000 cm^{-1}, and $E_{00}(2)$ = 21 000 cm^{-1}. The calculated absorption spectra (-·-) and the individual components (--) are also shown.

of α of the second excited state from the 500-cm^{-1} mode is larger and leads to a strong interference effect. Therefore, in order for deenhancement to occur, the displacement of the mode must be big in both excited states and in addition the ΔE and the ratio of μ's must be of the correct magnitude.

When both modes have big but different displacements (same sign) in the second excited state, the excitation profiles for both modes show strong interference effects. However, the relative intensities are different. For example, the excitation profiles for both modes show a very strong interference effect when the displacement is 5.0 for the 700 cm^{-1} and 3.5 for the 500 cm^{-1} in the second excited state. (The rest of the parameters are the same as those in Table I.) The relative intensity of the 700-cm^{-1} mode to that of the 500-cm^{-1} mode in the resonant region is much bigger compared to that when the displacements of the two modes are 1.0 in the second excited state.

Effect of Γ. Varying the value of Γ of the second excited state has only a small effect on the resonance Raman intensity of the first excited state if the separation of the two excited states is large. The energies of the local minima and maxima are about the same as Γ of the second excited state is varied. The Raman intensity in resonance with the first excited state does not strongly depend on Γ. The intensity in resonance with the second excited state increases as Γ of the second state decreases.

Resonance Deenhancement. When there is a second excited state near the state of interest, there will always be an interference effect, large or small. Resonance deenhancement is a special type of interference in which the resonance Raman excitation profile does not follow the shape of the absorption band of the state of interest and the minimum of the excitation profile occurs near the maximum of the absorption band. The origin of the resonance deenhancement is clearly shown in the previous discussion by considering the real and imaginary parts of α of the first and the second excited states. It will occur when (1) the two excited states are well-separated in energy, (2) the transition dipole moment of the second excited state has a magnitude that makes the magnitude of its α comparable to that of the excited state of interest, and (3) the displacements of the modes are significant in both the first excited and the second excited states.

B. Two Electronic Excited States Are Close in Energy, and the Transition Dipole Moments of the Two States Are Similar. When two excited states are close in energy, the real and imaginary parts of α of the second excited state that are added to those of the first state will include the maximum in the imaginary part and the sign change in the real part, as shown in Figure 1d. The interpretations of the interference effect in this case are not as simple as those for the case where two excited states are well-separated in energy because the real and imaginary parts are not slowly varying, smooth functions in the region of interest. Therefore, it is more difficult to state simple and general rules and the spectra will generally have to be interpreted on a case by case basis. In order to illustrate several of the important trends, the excitation profiles for two excited states that are separated by 1000 cm^{-1} are calculated.

Effect of μ. The magnitude of α of the second excited state is strongly dependent on the transition dipole moment as was discussed previously. As the transition dipole moment of the second excited state increases, the magnitude of α of the second excited state increases. In order to focus on the effect of μ, the displacements of the two modes and the damping factors in the two excited states are kept the same and only the ratio of the μ's of the two excited states is varied. Displacements of 1.0 for both the 700-cm^{-1} and 500-cm^{-1} modes and a damping factor of 700 cm^{-1} are used in the calculation.

The resonance Raman intensity of the first excited state relative to that of the second excited state increases as μ_1 relative to μ_2 increases. When $\mu_1^2:\mu_2^2$ = 1:10, the excitation profile is almost identical with that of the second excited state alone. The dashed line in Figure 7 shows the excitation profile for the 700 cm^{-1} when $\mu_1^2:\mu_2^2$ = 1:1.

Effect of Δ. As the displacement of a particular mode in the second excited state increases, the magnitude of α of the second excited state increases. The features in the excitation profiles arising from the interference are quite complicated, and no simple general rules are evident. In order to give an example of what can happen, the changes in the profiles caused by increasing the Δ's and keeping constant the ratio of the displacements of the two vibrational modes in the second excited state to those in the first excited state are calculated.

The excitation profile of the 700-cm^{-1} mode (—) is shown along with the absorption spectrum (-·-) in Figure 6a when the displacements in the second excited state are 0.5 for both modes and

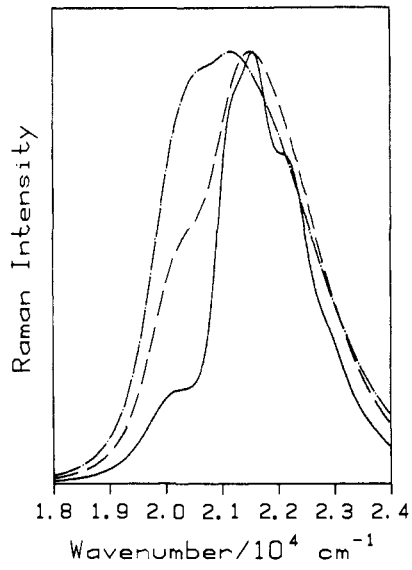

Figure 7. Effect of Γ on the excitation profiles of the 700-cm^{-1} mode when two electronic excited states are close in energy. The profiles are calculated for Γ = 400 cm^{-1} (—), 700 cm^{-1} (– –), and 1000 cm^{-1} (–·–). The displacements of the 500- and the 700-cm^{-1} modes in the two excited states are 1.0. $\mu_1^2:\mu_2^2$ = 1:1, $E_{00}(1)$ = 20 000 cm^{-1}, and $E_{00}(2)$ = 21 000 cm^{-1}.

in Figure 6b when the displacements in the second excited state are 1.5 for both modes. The rest of the parameters are the same as in Table I ($\mu_1^2:\mu_2^2$ = 1:1). The Raman intensity of the first excited state relative to that of the second excited state increases as the Δ's in the second excited state increase. The maxima of the excitation profiles do not exactly match those with one state alone. The maximum of the first excited state is shifted to lower energy relative to that of the excitation profile with one state only, whereas the maximum of the second excited state is shifted to higher energy. The relative intensities between modes remain the same as long as the ratio of the displacements of modes in the second excited state does not change. The interpretation of the cause of the interference effects that occur in this case is not as obvious as that for the case when the two electronic excited states are well-separated in energy and the higher state has a high transition dipole moment.

Effect of the Damping Factor Γ. The damping factor of the second excited state causes a more pronounced effect on the Raman excitation profiles when two states are close in energy than when they are well-separated. It is easy to understand the effect of the damping factor of the second excited state by considering the change in the magnitude of α depending on the damping factor. As the damping factor in the second excited state increases, the magnitude of α of the second excited state decreases and the interference from the second excited state to the total α decreases. Therefore, the dominance of the first excited state in the Raman intensity will increase as the damping factor of the second excited state increases. In order to focus the effect of the damping factor of the second excited state, all of the parameters are fixed except the damping factor of the second excited state. The excitation profiles for the 700-cm^{-1} mode are shown in Figure 7. The parameters used in this calculation are the same as in Table I except Γ is varied from 400 to 1000 cm^{-1} ($\mu_1^2:\mu_2^2$ = 1:1). The excitation profile shows a structure in the energy region corresponding to the second excited state as the damping factor decreases. In addition, the intensity in the first excited-state energy region relative to that in the second excited-state region increases as Γ increases as discussed previously.

IV. Application of the Theory

Four applications of the calculations of the excitation profiles are discussed below. The first two examples are the excitation profiles of $Co(en)_3^{3+}$ and $PdBr_4^{2-}$, which show strong resonance deenhancement.[14] Both complexes have a low-energy state that is well-separated in energy from a second state. In addition, the transition dipole moment of the second excited state is much higher than that of the first excited state. The third example is the excitation profiles of $Ru_2(O_2CCH_3)_4Cl$. In this example, the excitation profile of one of the modes shows very strong resonance deenhancement, but that of another mode does not.[21] This complex also has excited states that are well-separated in energy, and the transition dipole moment of the second excited state is much higher than that of the first excited state. The fourth example is the excitation profiles of $W(CO)_4$(*i*-PrDAB), which do not show any resonance deenhancement.[22] This complex has several excited states that are very close in energy and have similar transition dipole moments. The resonance Raman excitation profiles of all of these complexes are calculated by using the time-dependent theory as described previously. For simplicity, only two electronic excited states are considered in all of the complexes. The resonance Raman excitation profiles are calculated for a given set of values, Δ_k, ω_k, ω_l, Γ, μ_r, and $E_{00}(r)$ for two electronic excited states by use of eqs 2–4. Only one set of parameters is used for each complex to calculate the resonance Raman excitation profiles.

The values of many of the parameters are severely constrained or even uniquely determined by the experimental observables. The values of the μ's for each excited state involved can be obtained from the experimental absorption spectrum when the bands are resolved. The values of the E_{00}'s can be estimated from the absorption spectrum. When the bands are smooth, it is difficult to obtain the exact values of the E_{00}'s, but the values can usually be estimated to within an accuracy of several hundred reciprocal centimeters.

The ratio of the Δ's can in principle be accurately determined from the resonance Raman intensities if the ratio of the Δ's in the second excited electronic state is the same as that in the first. Because the ratios will usually be different, the resonance Raman intensities can only be used to provide a reasonable first estimate as a starting point for the fitting. In addition, if the two states have very different magnitudes of μ, then the Δ's determined from the Raman intensities in the region of resonance with the state with the biggest μ will be relatively accurate for that state even if the ratios change because that state will dominate the excitation profiles. The magnitudes of the Δ's can in principle be determined from the widths of the absorption bands by using eq 6,[23,24] where

$$2\sigma^2 = \sum_k \Delta_k^2 \omega_k^2 \qquad (6)$$

$2\sigma^2$ is the width of the electronic absorption spectrum at $1/e$ of the height. This equation will be useful when only one normal mode is highly displaced. When many modes are displaced, it will provide an upper limit to the sums of the displacements. These considerations provide experimentally determined constraints and limits on the values of Δ to be used in the fitting.

The value of Γ cannot be uniquely determined from the experimental data discussed in this paper. An upper limit to its value can be determined from the widths of vibronic features in an absorption spectrum or excitation profile.[25-28] If the bands are broad and featureless, it is not possible to estimate the value of Γ because the smooth envelope may be caused by a large Γ, by inhomogeneous broadening that can be treated as a weighted superposition of sharp line spectra, each of which has a small value of Γ, or by a combination of both. An upper limit to Γ may also be determined from the relative intensities of overtone bands to fundamentals in the resonance Raman spectra.[3] It is also extremely important to note that the inclusion of additional normal modes in a calculation act like the damping factor and their effects are often hidden in it. Thus, the larger the number of modes that are included in the calculation, the smaller the value of Γ required

(23) Zink, J. I. *Coord. Chem. Rev.* **1985**, *64*, 93.
(24) Heller, E. J.; Sundberg, R. L.; Tannor, D. *J. Phys. Chem.* **1982**, *86*, 1822.
(25) Yoo, C. S.; Zink, J. I. *Inorg. Chem.* **1983**, *22*, 2474.
(26) Larson, L. J.; Zink, J. I. *Inorg. Chem.* **1989**, *28*, 3519.
(27) Hollingsworth, G. J.; Shin, K. S. K.; Zink, J. I. *Inorg. Chem.* **1990**, *29*, 2501.
(28) Tutt, L.; Zink, J. I. *J. Am. Chem. Soc.* **1986**, *108*, 5830.

to give a smooth absorption band or excitation profile.[3] The inclusion of these modes with small distortions will not have a large effect on the calculated values of Δ for the modes that have large displacements and show the largest interference effects. However, they will have a nonnegligible effect on Γ. This effect may also prevent the exact value of Γ from being determined. The importance of the effects of the number of modes used in the calculation on the value of Γ is explicitly illustrated in the application of the theory to $Co(en)_3^{3+}$ discussed below. For all of the above reasons, Γ is treated in this paper as a phenomenological damping factor, which includes the effects of the "bath" and of other modes.

The first two examples discussed below have also been treated by using the KHD formalism.[14] In the KHD treatment, the parameters were the difference in energy between the E_{00}'s, the line width, and a parameter that consolidates all of the other molecular properties including the μ's and the sum of the Franck–Condon factors.

Application 1. $Co(en)_3^{3+}$. Resonance Deenhancement When Two Excited States Are Well-Separated in Energy and the Transition Dipole Moment of the Second Excited State Is Much Higher Than That of the First Excited State. Resonance deenhancement was first recognized in the excitation profiles of this molecule by Spiro et al.[14] It is a good molecule for applying the time-dependent theory because most of the parameters are constrained. The E_{00}'s, μ's, and bandwidths of each state are known from the absorption spectrum. E_{00} is 18 500 cm^{-1} for the first excited state and 39 000 cm^{-1} for the second excited state used in the calculation. The observed molar absorptivities are 96 for the first excited state and 17 500 for the second excited state.

Two totally symmetric modes, the 280-cm^{-1} ligand–ring deformation mode and the 526-cm^{-1} Co–N stretching mode, are used in the calculation. (Two non totally symmetric modes, the 376-cm^{-1} T_{2g} Co–N bend and the 444-cm^{-1} E_g Co–N stretching modes, do not show any resonance enhancement or deenhancement.) The ratio of the Δ's of the modes in the first excited state were estimated from the resonance Raman intensity, and the absolute magnitudes of the Δ's were determined from the width of the absorption band. The experimental Raman intensities of the modes in resonance with the second excited state are not available. Therefore, the same ratio of the Δ's as that of the first excited state was used for the second excited state. The absolute magnitude of the Δ's was also determined from the width of the absorption band of the second excited state. The displacements are 2.2 for the 526-cm^{-1} mode and 3.5 for the 280-cm^{-1} mode in the first excited state. Γ is 800 cm^{-1}. These parameters give the calculated absorption band of the first excited state whose peak maximum and the full width at half-maximum are 21 450 and 3460 cm^{-1}, respectively. The experimentally observed values are 21 500 and 3500 cm^{-1}, respectively. The displacements are 4.0 for the 526-cm^{-1} mode and 5.78 for the 280-cm^{-1} mode in the second excited state. Γ is 3000 cm^{-1}. These parameters give the calculated absorption band of the second excited state whose peak maximum and the full width at half-maximum are 47 900 and 8530 cm^{-1}, respectively. The experimentally observed values are 47 400 and 9000 cm^{-1}, respectively.

The excitation profiles are calculated in six steps: (1) initial values of the parameters are determined from the Raman and absorption spectra; (2) the overlap for each excited state is calculated by using eq 2; (3) the total overlap is calculated by summation of the overlaps of the individual excited states; (4) the resonance Raman cross section is calculated from the half Fourier transform of the total overlap (eq 3); (5) the resonance Raman intensity is calculated by using eq 4; (6) the ratio of the μ's is varied to obtain the best fit to the experimental excitation profiles. Only one set of the parameters is used in the calculation to obtain the excitation profiles of the two modes.

The excitation profiles of best fit for the 280-cm^{-1} (---) and 526-cm^{-1} (—) modes in the energies between 16 000 and 22 000 cm^{-1} are shown in Figure 8. They are calculated by using the parameters given above. The ratio of the μ's was varied to obtain the best fit to the experimental data. $\mu_1^2:\mu_2^2$ = 1:110 for the calculated excitation profiles shown in Figure 8. The calculated

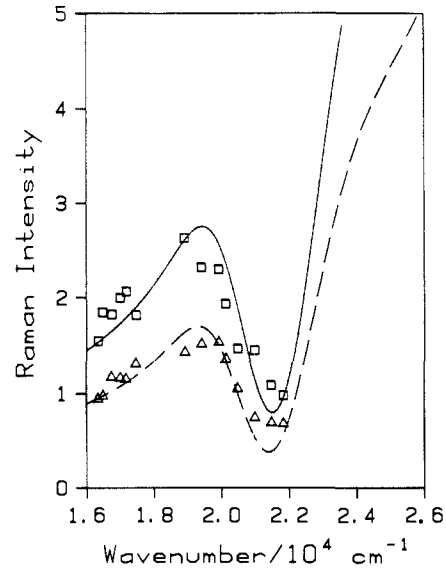

Figure 8. Calculated and experimental excitation profiles for $Co(en)_3^{3+}$ illustrating the resonance deenhancement. The solid line is the calculated excitation profile and the squares are the experimental data points for the 526-cm^{-1} mode, and the dashed line and the triangles are those for the 280-cm^{-1} mode, respectively. The values of the parameters for the first excited state are the following: Δ for the 526-cm^{-1} mode, 2.2; Δ for the 280-cm^{-1} mode, 3.5; E_{00}, 18 500 cm^{-1}; Γ, 800 cm^{-1}. The values of the parameters for the second excited state are as follows: Δ for the 526-cm^{-1} mode, 4.0; Δ for the 280-cm^{-1} mode, 5.78; E_{00}, 39 000 cm^{-1}; Γ, 3000 cm^{-1}. $\mu_1^2:\mu_2^2$ = 1:110.

profiles are compared with the experimental values. The calculated excitation profiles for both modes reproduce the resonance deenhancement well. The minima occur at ~21 500 cm^{-1}, which is the maximum of the absorption band. The local maxima occur at ~19 300 cm^{-1} for both modes. Not only is the experimental bandwidth and band shape of each excitation profile reproduced in the calculation, but also the relative intensities between the two profiles are reproduced as well. It is important to note that the relative intensities of the excitation profiles of the two modes are sensitive to the ratio of the displacements in the second excited state.

The values of the phenomenological damping factor Γ in the first and second excited states that are used in the above calculations are large because the effects of other modes and of inhomogeneous broadening have not been included. However, inclusion of the latter two effects does not significantly affect the calculations. For example, the calculated resonance Raman excitation profile for the 280-cm^{-1} mode with Γ = 100 cm^{-1} in both the first and the second excited states is shown in Figure 9a. All of the other parameters are the same as those used to obtain the fit to the experimental data shown in Figure 8. (The calculated profile from Figure 8 is shown in Figure 9c to facilitate comparison.) Resolved vibronic structure is seen on the calculated profile, but the overall shape and the positions of the local minimum and maximum are unchanged. The vibronic structure would probably not be recognized in the experimental data, given the separation of the data points and the experimental uncertainty of the intensity measurements. Inhomogeneous broadening smears out the vibronic structure as shown in Figure 9b. The inhomogeneously broadened profile is calculated by taking the Gaussian-weighted superposition of the structured profiles, each with an energy offset.[29] The calculated profile in Figure 9b uses an inhomogeneous bandwidth of 200 cm^{-1} fwhm.

Inclusion of additional modes will act like a damping factor and "wash out" the structure as was discussed previously. For example, the excitation profile calculated with the inclusion of just two additional modes, the 444-cm^{-1} metal–ligand mode and the 1470-cm^{-1} ethylenediamine mode, contains barely discernible

(29) Reber, C.; Zink, J. I. Manuscript in preparation.

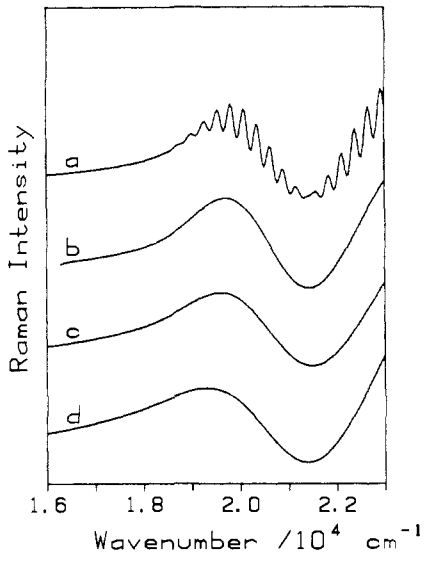

Figure 9. Calculated and experimental excitation profiles for the 280-cm^{-1} mode of $Co(en)_3^{3+}$ illustrating the effects of Γ and of the inclusion of inhomogeneous broadening and of additional modes on the deenhancement: (a) excitation profile calculated by using Γ = 100 cm^{-1} in both excited states and the same values of the other parameters as were used in Figure 8; (b) excitation profile from part a with the inclusion of inhomogeneous broadening; (c) best fit profile from Figure 8; (d) profile calculated by including two additional modes. The profiles are offset for clarity.

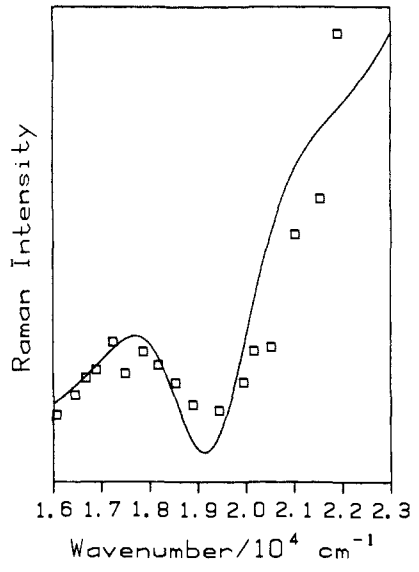

Figure 10. Calculated and experimental excitation profiles for $PdBr_4^{2-}$ illustrating the resonance deenhancement. The solid line is the calculated excitation profile, and the squares are the experimental data points for the 192-cm^{-1} mode. The values of the parameters for the first excited state are the following: Δ for the 192 cm^{-1} mode, 4.0; E_{00}, 17 500 cm^{-1}; Γ, 1200 cm^{-1}. The values of the parameters for the second excited state are as follows: Δ for the 192-cm^{-1} mode, 5.45; E_{00}, 37 500 cm^{-1}; Γ, 1200 cm^{-1}. $\mu_1^2:\mu_2^2$ = 1:55.

structure and is almost identical with the best fit profile. This profile, shown in Figure 9d, was calculated by using Γ = 100 cm^{-1} in both the first and second excited states, experimentally determined $\mu_1^2:\mu_2^2$ = 1:180, and the same values for all of the other parameters as were used in Figure 8. These results show that the essential features of the resonance deenhancement profiles can be calculated either by including more modes and using smaller values of Γ or by using a small number of modes for which detailed excitation profile data are available and lumping the effects of the other modes into the phenomenological damping factor. The latter strategy is adopted for the remaining applications discussed in this paper.

The calculation provides information about the molecule in the excited state. First, the strong resonance deenhancement for both modes in the energy region in resonance with the first excited state shows that the 526- and the 280-cm^{-1} modes are strongly involved in the second excited state as well as in the first excited state. Second, in the process of excitation into the first excited state, the calculated Co–N bond length change in $Co(en)_3^{3+}$ is 0.044 Å.[30] However, the displacements in the first and the second excited states used in the calculation are not uniquely determined because the experimental resonance Raman spectrum in the energy region of the second excited state is not known. The relative Raman intensities of the modes in the energy region of the first excited state are greatly influenced by the displacements in the second excited state. Therefore, the calculated displacements for the first excited state obtained from the resonance Raman intensity are not unambiguously determined although the values are reasonable.[31]

Application 2. $PdBr_4^{2-}$. Resonance Deenhancement When Two Excited States Are Well-Separated In Energy and the Transition Dipole Moment of the Second Excited State Is Much Higher Than That of the First Excited State. The excitation profile for the 192-cm^{-1} mode of $PdBr_4^{2-}$ shows strong resonance deenhancement in the energy region of the weak (ϵ = 250 M^{-1} cm^{-1}) absorption band at 19 600 cm^{-1}.[14] Two stronger absorption bands occur to higher energy at 30 100 (ϵ = 11 500 M^{-1} cm^{-1}) and 40 400 cm^{-1} (28 900 M^{-1} cm^{-1}).[32] The excitation profile for the 192-cm^{-1} mode is calculated by using the procedure described above. All of the parameters used in the calculation were obtained from the experimental data.

The parameters for the first excited state were obtained from the width of the absorption band of the first excited state. Only the 192-cm^{-1}, totally symmetric Pd–Br stretch is considered in the calculation because it is the only mode that shows the resonance effect. The displacement of the 192-cm^{-1} mode in the first excited state is 4.0. E_{00} is 17 500 cm^{-1}, and Γ is 1200 cm^{-1}. The absorption band of the first excited state calculated by using these parameters has a peak maximum and full width at half-maximum of 19 100 and 3000 cm^{-1}, respectively. The experimentally observed values are 19 600 and 2950 cm^{-1}, respectively.[32]

The second excited state that was used to calculate the interference effect is the absorption band at 40 400 cm^{-1}. The parameters for this excited state were also obtained from the bandwidth. The displacement of the 192-cm^{-1} mode in the second excited state is 5.45. E_{00} is 37 500 cm^{-1}, and Γ is 1200 cm^{-1}. The absorption band calculated from these parameters has a peak maximum at 40 350 cm^{-1} and full width at half-maximum of 3400 cm^{-1}. The experimentally observed values are 40 400 and 4190 cm^{-1}, respectively.[32]

The excitation profile of best fit for the 192-cm^{-1} mode in the energy region of the first excited state between 16 000 and 23 000 cm^{-1} is shown in Figure 10. The ratio of μ's was varied to obtain the best fit to the experimental data. $\mu_1^2:\mu_2^2$ = 1:55 for the calculated excitation profile shown in Figure 9. The calculated excitation profile is superimposed on the experimental values. The calculated excitation profile shows the resonance deenhancement very well and is a good fit to the entire profile.

Many unsuccessful attempts were made to fit the experimental profiles by considering two absorption bands at 19 600 and 30 000

(30) The formula to convert the dimensionless displacement Δ into angstroms is $\delta = [((6.023 \times 10^{23})/m)(\hbar/2\pi c\omega)]^{1/2}10^8\Delta$, where m is the mass involved in the vibration (gram atomic weight) (e.g., C = 12 g), ω is the wavenumber of the vibrational mode (cm^{-1}), $\hbar = h/2\pi$ where h is Planck's constant (g cm^2 s^{-1}), c is the speed of light (cm s^{-1}), δ is the displacement (Å), and Δ is the dimensionless displacement. The mass used to convert the dimensionless Δ into angstrom unit for ν(Co–N) is half of the mass of the ethylenediamine group. Because the normal coordinate involves the motion of six nitrogen atoms, the factor $1/\sqrt{6}$ is multiplied by the value of normal-coordinate displacement to calculate the individual Co–N bond length change.

(31) Wilson, R. B.; Solomon, E. I. *J. Am. Chem. Soc.* **1980**, *102*, 4085.

(32) Rush, R. M.; Martin, D. S.; LeGrand, R. G. *Inorg. Chem.* **1975**, *14*, 2543.

cm^{-1}. The parameters for the lowest excited state were the same as described above. The parameters for the second excited state were determined from the width of the absorption band at 30100 cm^{-1}. The displacement of the 192-cm^{-1} mode is 4.0. E_{00} was 28000 cm^{-1}, and the damping factor was 1200 cm^{-1}. The absorption band calculated from these parameters had its peak maximum at 29550 cm^{-1} and a full width at half-maximum of 3000 cm^{-1}, which are in good agreement with the experimentally observed values of 30200 and 2960 cm^{-1}, respectively. No satisfactory fits to the experimental excitation profile could be obtained. The calculated profile reproduced the minimum and showed a very good fit to the higher energy region. However, the calculated local maximum occurred at about 1000 cm^{-1} higher in energy than that of the experimental excitation profile, and the calculated intensity in the lower energy region was too small.

It is possible that the interference effect in this system arises from a combination of both the 30100- and 40400-cm^{-1} absorption bands. It is easy to include three excited states in the calculation by using the time-dependent theory. However, inclusion of three states introduces another set of parameters, and the interpretation becomes less physically meaningful.

The two calculations shown above provide information about the molecule in its excited states. First, in the process of excitation into the lowest excited state, the Pd–Br bond length change is 0.094 Å. The mass used to convert the dimensionless Δ into angstrom units for ν(Pd–Br) is the mass of bromine atom.[30] Because the normal coordinate involves the motion of four Br atoms, the individual Pd–Br bond length change is $1/\sqrt{4}$ of the normal-coordinate change. The Pt–Br bond length change in the lowest excited state of an analogous compound, $PtBr_4^{2-}$, is estimated to be 0.095 Å.[33] Second, the strong resonance deenhancement for the ν(Pd–Br) mode in the lowest excited state shows that the ν(Pd–Br) mode is strongly involved not only in the lowest excited state but also in the higher excited state. The displacements obtained from the widths of the absorption bands are uniquely determined because only one mode contributes to the widths.

Application 3. $Ru_2(O_2CCH_3)_4Cl$. Effect of Small Δ's in the Second Excited State. Detailed excitation profiles for this molecule including the excitation profiles for two fundamentals, one overtone, and one combination band have been published.[21] There are two especially interesting features in this example. First, the excitation profile for the 372-cm^{-1} mode, ν_2(Ru–O), shows strong resonance deenhancement but those for the 330-cm^{-1} mode, ν_1(Ru–Ru), the first overtone, $2\nu_1$, and the combination, $(\nu_1 + \nu_2)$, do not. As described in section III, this interesting feature can occur when one of the modes has a big displacement in the second excited state and the other does not. Second, resonance deenhancement occurs even though both excited states under consideration result from allowed transitions.

The first excited state was assigned to an electric dipole allowed π(Ru–O, Ru_2) → $\pi^*(Ru_2)$ transition.[34] The absorption band's maximum occurs at 21600 cm^{-1}. E_{00} is 17200 cm^{-1}. The displacements in the first excited state are 3.1 and 2.1 for ν_1 and ν_2, respectively. The damping factor is 1600 cm^{-1}. The second excited state arising from a strongly allowed Cl → $\pi^*(Ru_2)$ transition gives a band in the UV region with E_{00} at 30000 cm^{-1}. The ratio of Δ's of the two modes in the second excited state could not be obtained because no Raman intensities are available. Therefore, the displacements of the two modes are determined by fitting the excitation profiles. The observed molar absorptivities are 1000 for the lowest excited state and 9300 for the higher excited state. The bandwidth and maximum of the second excited state were not measured for the acetate complex but were 4210 and 33780 cm^{-1}, respectively, for the propionate complex.[34]

The excitation profiles for the best fit to ν_1, ν_2, $2\nu_1$, and $(\nu_1 + \nu_2)$ of $Ru_2(O_2CCH_3)_4Cl$ in the energies between 15000 and 23000 cm^{-1} are compared with the experimental data in Figure 11. They are calculated by using the displacements of 0.4 for ν_1 and 2.2 for ν_2 in the second excited state, and $\mu_1^2:\mu_2^2 = 1:9.5$. The calculated excitation profile for the ν_2 band shows strong deenhancement at about 20500 cm^{-1}. Those for the ν_1, $2\nu_1$, and $(\nu_1 + \nu_2)$ bands do not show deenhancement. The experimental bandwidth and band shape of each excitation profile are accurately reproduced in the calculation. In addition, the relative intensities between each profile are accurately reproduced although the calculated intensity of the combination band $(\nu_1 + \nu_2)$ is slightly overestimated. (All calculated excitation profiles are normalized to the maximum of the ν_1 band.) The maxima of the excitation profiles of the ν_1, $2\nu_1$, and $(\nu_1 + \nu_2)$ bands are at 20000 cm^{-1}, which is near the maximum of the electronic absorption band in resonance. The minimum of the excitation profile of the ν_2 band occurs at 20500 cm^{-1}, near the maximum of the electronic absorption band in resonance.

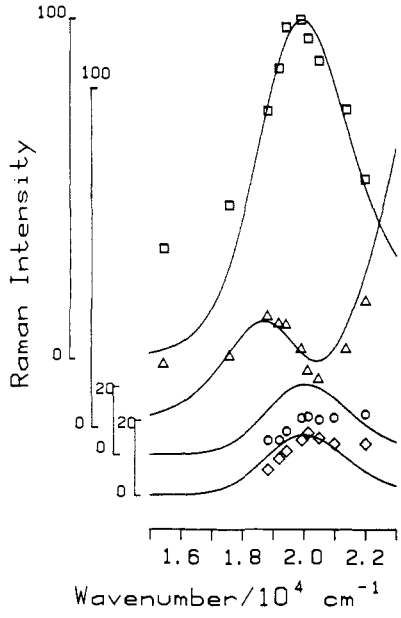

Figure 11. Calculated and experimental excitation profiles for $Ru_2(O_2CCH_3)_4Cl$ illustrating the effect of Δ in the second excited state. The solid lines are the calculated excitation profiles, and the symbols are the experimental data points for ν_1, ν_2, $(\nu_1 + \nu_2)$, and $2\nu_1$ (top to bottom). The values of the parameters for the first excited state are the following: Δ for ν_1, 3.1; Δ for ν_2, 2.1; E_{00}, 17200 cm^{-1}; Γ, 1600 cm^{-1}. The values of the parameters for the second excited state are as follows: Δ for ν_1, 0.4; Δ for ν_2, 2.2; E_{00}, 30000 cm^{-1}; Γ, 1600 cm^{-1}. The $\mu_1^2:\mu_2^2$ ratio is 1:9.5.

The calculation of the excitation profiles of $Ru_2(O_2CCH_3)_4Cl$ shows several interesting features. First, the excitation profiles for the ν_1 band and the first overtone of that mode do not show strong resonance deenhancement. The reason for the absence is the small displacement of the mode in the second excited state compared to that of the first excited state. This small displacement is consistent with the Cl → $\pi^*(Ru_2)$ charge-transfer assignment. The electron originates from an orbital on the Cl^- instead of a Ru–Ru bonding orbital. Therefore, the displacement is smaller. Second, the excitation profile for the ν_2 band shows strong deenhancement because the displacements of the mode in both the first and the second excited state are big. This big displacement is also consistent with the Cl → $\pi^*(Ru_2)$ charge transfer because the decrease in formal charge on the Ru results in a weaker Ru–O interaction. Third, the excitation profile of the $(\nu_1 + \nu_2)$ combination band in which one of the components has a big displacement in the second excited state and the other has a small displacement in that state does not show strong resonance deenhancement. Fourth, these results show that resonance deenhancement can occur when two allowed transitions interfere. A forbidden transition is not a requirement for a resonance deenhancement. As described earlier, resonance deenhancement will occur if the displacement of a mode is big in both excited states and the ΔE and the ratio of μ's are of the correct magnitude to make the magnitude of α of the higher excited state comparable

(33) Yersin, H.; Otto, H.; Zink, J. I.; Gliemann, G. *J. Am. Chem. Soc.* **1980**, *102*, 951.
(34) Miskowski, V.; Gray, H. B. *Inorg. Chem.* **1988**, *27*, 2501.

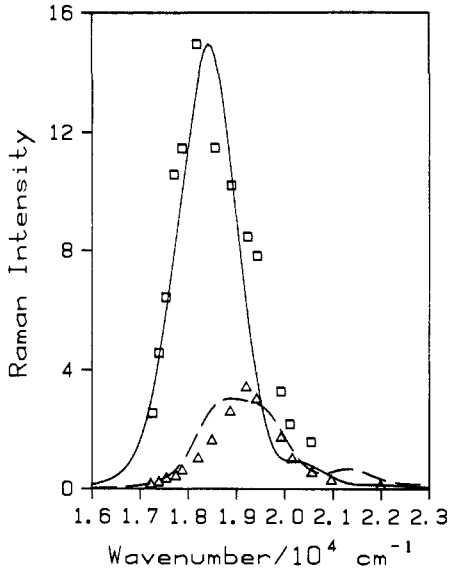

Figure 12. Calculated and experimental excitation profiles for W(CO)$_4$(*i*-PrDAB) illustrating the effect of two close-lying excited states. The solid line and dashed lines are the calculated excitation profiles, and the symbols are the experimental data points for the 230-cm^{-1} mode (□) and the 1482-cm^{-1} mode (Δ). The values of the parameters for the first excited state are the following: Δ for the 230-cm^{-1} mode, 3.0; Δ for the 1482-cm^{-1} mode, 0.05; E_{00}, 17 200 cm^{-1}; Γ, 500 cm^{-1}. The values of the parameters for the second excited state are as follows: Δ for the 230-cm^{-1} mode, 1.5; Δ for the 1482-cm^{-1} mode, 0.9; E_{00}, 18 200 cm^{-1}; Γ, 500 cm^{-1}. $\mu_1^2:\mu_2^2$ = 1:0.5.

to that of the excited state of interest.

Application 4. W(CO)$_4$(*i*-PrDAB). Interference Effects When Two Electronic States Are Close in Energy and the Transition Dipole Moments of the Two States Are Similar. The metal–ligand charge-transfer bands of many metal–α-diimine complexes are composed of several overlapping bands having similar transition dipole moments.[22,35] The spectrum of the isopropyldiazabutadiene (DAB) complex chosen here is typical.[22] Excitation profiles were reported for two highly displaced normal modes, a 230-cm^{-1} W–N stretch and a 1482-cm^{-1} C–N stretch.[22] Both modes show strong resonance enhancement, but the maxima in the excitation profiles occur at two different wavenumbers even though only one broad absorption band is observed. To illustrate how these effects can be caused by the presence of two nearby electronic excited states, the experimental spectra are fit by a two electronic excited state and two vibrational mode model. Because the two absorption bands overlap, the parameters used in the calculation were obtained by fitting the excitation profiles to the experimental data.

E_{00} of the first excited state used in the calculation is 17 200 cm^{-1}. The displacements in the first excited state are 3.0 and 0.05 for the 230- and the 1482-cm^{-1} modes, respectively. E_{00} of the second excited state is 18 200 cm^{-1}. The displacements in the second excited state are 1.5 and 0.9 for the 230- and the 1482-cm^{-1} modes, respectively. The damping factors for both excited states are 500 cm^{-1}. The $\mu_1^2:\mu_2^2$ ratio used in the calculation is 1:0.5.

The excitation profiles of best fit for the 230- (—) and the 1842-cm^{-1} modes (- - -) are shown in Figure 12. These are calculated by using the parameters given above. The calculated and experimental excitation profiles are in good agreement. The maximum of the calculated excitation profile for the 230-cm^{-1} mode occurs at 18 500 cm^{-1}, whereas that of the 1482-cm^{-1} mode occurs at 19 200 cm^{-1}. The bandwidths of the excitation profiles and the relative intensities of each profile are reproduced well in the calculation.

This calculation shows that the presence of two excited states contributing to one smooth absorption band can cause the maxima in the excitation profiles of different modes to have different energies. Two vibrational modes are displaced differently in these two excited states. The magnitude of the displacement of the 1482-cm^{-1} mode in the first excited state is much smaller than that in the second excited state, whereas the displacement of the 230-cm^{-1} mode is larger in the first excited state than in the second excited state. This difference in displacement and the closeness of the two states give rise to the different maxima in the excitation profiles for the two modes. The displacements used in this calculation illustrate how these effects can arise and provide new guidelines for interpreting the profiles. They are probably not unique because not enough experimental information can be obtained about each of the individual overlapping bands that contribute to the broad absorption.

V. Conclusions

The presence of two or more excited states can strongly affect the Raman intensity measured in resonance with one of the states. The effect is interpreted by examining the real and the imaginary parts of the Raman scattering cross section α. The time-dependent theory provides a simple method of calculating α and allows explicit effects of μ, Δ, and E_{00} to be examined. General trends are derived from model calculations. The theory is applied to molecular examples that illustrate the general trends. Spectroscopic properties of the molecules including the distortions and their consistency with known orbital assignments are interpreted.

Acknowledgment. The support of the NSF (Grant CHE88-06775) is gratefully acknowledged.

(35) (a) Balk, R. W.; Stufkens, D. J.; Oskam, A. *Inorg. Chim. Acta* **1978**, *28*, 133. (b) Balk, R. W.; Stufkens, D. J.; Oskam, A. *Inorg. Chim. Acta* **1979**, *34*, 267. (c) Balk, R. W.; Stufkens, D. J.; Oskam, A. *J. Chem. Soc., Dalton Trans.* **1982**, 275. (d) Dijk, H. K. V.; Servaas, P. C.; Stufkens, D. J.; Oskam, A. *Inorg. Chim. Acta* **1985**, *104*, 4494.